Metrics to Evaluate Compression Algorithms for Raw SAR Data

Chané Pieterse[1*], Warren P. du Plessis [1], Richard W. Focke [2]

[1] Department of Electrical, Electronic and Computer Engineering, University of Pretoria, Pretoria, 0002, South Africa
[2] Radar and Electronic Warfare Sytems, Defence, Peace, Safety and Security, Council for Scientific and Industrial Research (CSIR), Meiring Naude Road, Pretoria, South Africa
[*]chanepieterse09@gmail.com

Abstract: Modern SAR systems have size, weight, power and cost (SWAP-C) limitations since platforms are becoming smaller while SAR operating modes are becoming more complex. Thus, SAR systems are producing an ever-increasing volume of data that needs to be transferred to a ground station for processing. A compression algorithm seeks to reduce the data volume of the raw data; however, the algorithm can cause degradation and losses that may degrade the effectiveness of the SAR mission.
This work addresses the lack of standardised quantitative performance metrics so that the performance of SAR data-compression algorithms can be objectively quantified. Therefore, metrics are established in two different domains, namely the data domain and the image domain. Since different levels of degradation are acceptable for different SAR applications, a trade-off can be made between the data reduction and the degradation caused by the algorithm. Due to SWAP-C limitations there remains a trade-off between the performance and the computational complexity of the compression algorithm.

1. Introduction

Synthetic aperture radar (SAR) is the only imaging system that can provide high-resolution images of wide areas in all weather conditions, during the day or night [1], [2]. Other advantages of SAR are that it provides information that is complementary to optical images and certain frequencies have penetration capabilities which allow much more information to be extracted from a scene [2]. Therefore, SAR has been used for various military, commercial and earth observation applications for the past three decades [1], [2]. In the case of military applications, SAR technology is increasingly being used in unmanned aerial vehicle (UAVSAR) systems [3], [4], while for earth observation applications, satellites are being equipped with higher resolution SARs while the platforms are becoming smaller and lighter [5]. In both cases SWAP-C play an important role in the system design.

Not only are platforms becoming smaller, but SAR technology is moving towards being multi-band, multi-polarized, having very high resolution and also having multiple operating modes. All of these factors contribute to SAR systems producing an ever-increasing volume of data, so despite technological advances, the on-board storage and downlink bandwidth remain limiting factors [6], [7]. Due to the limited SWAP-C of many platforms, minimal processing can be performed on board, and thus the data need to be transferred to a ground station for processing. In order to accommodate the downlink and storage limitations, the raw SAR data must be compressed [7]. The objective of the compression algorithm is thus to reduce the data produced by the SAR to as few bits as possible, while using only limited processing and preserving the information content.

Various compression algorithms have been investigated, including the block adaptive quantiser (BAQ) [8], [9] and variations thereof [6], [10], [11], vector quantisation (VQ) [9], [12], transform coding [13], trellis coded quantisation [14], wavelets [15], compressive sensing [16], predictive coding [17], coding after range focusing [14], as well as combinations of more than one algorithm [18]. The de facto standard is the BAQ [6], [19] which utilizes a Lloyd-Max quantiser [20], [21] to exploit the fact that the in-phase (I) and quadrature (Q) components can be assumed to follow Gaussian distributions with zero mean [8], [9]. More advanced variations of this method have been implemented on new SAR systems as processing capabilities improve [7], but the underlying BAQ algorithm is still being used.

A compression algorithm seeks to reduce the data volume to solve the problem of transmitting and/or storing the raw data. However, any degradation and loss that the algorithm causes should also be determined as a low quality SAR image may degrade the effectiveness of the SAR mission. Therefore, the compression algorithm must be evaluated to determine both whether it is effective in reducing the data volume as well as how significant the associated image-quality losses that occurred are.

Despite the importance of being able to quantify the performance of SAR data-compression algorithms, there does not appear to be a widely-accepted set of metrics for this purpose. The problem is compounded by the fact that different publications on SAR data compression often propose new metrics to emphasise the unique benefits of the proposed algorithms (e.g. [12] and [17]). This lack of standardised quantitative performance metrics means that the performance of SAR data-compression algorithms cannot be objectively quantified.

A critical evaluation of a number of SAR compression performance metrics is provided to overcome this difficulty. No single metric is suitable because the relative importance of each factor will differ depending on each system's unique requirements, so a number of metrics which quantify different aspects of SAR data compression performance are evaluated. These metrics consider how significantly the data rate is reduced, the loss of information, and the processing required for compression. Furthermore, the metrics evaluated consider both the data domain, where compression and decompression are performed, and the image domain, where the final SAR output is produced [6], [10], [22].

The metrics in the data and image domains are discussed in Sections 2 and 3, respectively. SAR applications and the specific metrics of importance for each application

are considered in Section 0. The metrics are applied to the compression of various data sets in Section 5, and a brief conclusion is provided in Section 6.

2. Data-Domain Metrics

The metrics that can be used to evaluate the efficiency of the compression algorithm in the data domain are established below. As can be seen in Fig. 1, these metrics are evaluated after decompressing the compressed data, except for the compression ratio (CR) which is computed directly after compressing the raw data. These metrics are used to determine the performance of the compression algorithm and the associated losses or errors it induces in the raw data samples. In some of the literature on raw SAR compression algorithms, the only metric used in this domain is the CR (e.g. [13], [18], [19]). Although compression ratio is an important metric, as it determines the data reduction, other metrics that evaluate the losses or errors associated with the algorithm are useful when investigating different compression algorithms. Some studies in the field of raw SAR data compression evaluate the signal-to-quantisation noise ratio (SQNR) in the data domain since it is the most widely used metric to measure the performance of a quantiser [17], [23], [24]. The effects that quantisation has on the image domain results are not considered in the data domain since SAR processing first needs to be performed. The following metrics are suggested to thoroughly evaluate the compression algorithm in the data domain.

2.1. Data Reduction Measure

- Compression Ratio

The compression ratio (CR) is defined as [9]

$$CR = \frac{Number\ of\ bits\ of\ the\ original\ data}{Number\ of\ bits\ of\ the\ compressed\ data}. \quad (1)$$

The CR indicates how efficiently the compression algorithm has reduced the data volume of the original data.

2.2. Statistical Parameters

Analysing the statistical parameters of each data set, with and without compression applied, can highlight changes that occurred in the statistical characteristics of the data due to the compression [10], [22]. A significant change in the statistical parameters in this domain means the compression algorithm was not as effective as it ideally could have been, since it corrupted the statistics of the original data. Note that each metric is evaluated for the uncompressed and decompressed data sets to compare the results. Also note that all statistical parameters, except the dynamic range, are computed for both the magnitude and phase components of the complex data.

- Dynamic Range

The dynamic range is the ratio between the largest and smallest values that the data can represent and is defined as

$$DR = \frac{Maximum\ value\ of\ data}{Minimum\ value\ of\ data}. \quad (2)$$

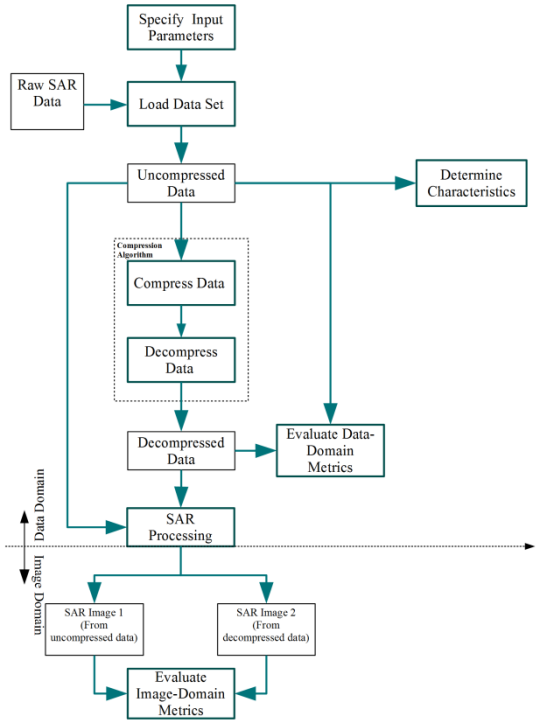

Fig. 1. *Process flow diagram*

The dynamic range is computed using the magnitude component, and not the phase component. A reduction in the dynamic range leads to an improved compression ratio as fewer bits are required to represent the data.

- Mean (First order statistic)

The mean, μ, is defined as [25]

$$\mu = \frac{\sum_{i=1}^{N}(X_i)}{N} \quad (3)$$

where X_i is the signal sample and N is the number of samples.

- Standard Deviation (Second order statistic)

The standard deviation,σ, is a measure of the variation of the data from the mean and is defined as [25]

$$\sigma = \sqrt{\frac{\sum_{i=1}^{N}(X_i-\mu)^2}{N-1}}. \quad (4)$$

- Skewness (Third order statistic)

The skewness, s, is a measure of how symmetrical the data are around the mean and is defined as [25]

$$s = \frac{\frac{1}{N}\sum_{i=1}^{N}(X_i-\mu)^3}{\left(\frac{1}{N}\sum_{i=1}^{N}(X_i-\mu)^2\right)^3}. \quad (5)$$

Certain compression algorithms, like the BAQ, exploit the fact that the I and Q components of raw SAR data follow a Gaussian distribution [8], [9]. In turn this means that the

amplitude component follows a Rayleigh distribution, while the phase component is uniformly distributed between $-\pi$ and π [26]. The skewness of a Rayleigh distribution and a uniform distribution are 0.63 and 0, respectively. Therefore, these values for the skewness can be used as a measure of how well the data components follow the applicable distributions. Skewness can thus be used to determine how much the compression algorithm caused the data to deviate from the distributions of the uncompressed data components.

- Kurtosis (Fourth order statistic)

The kurtosis, k, is a measure of how outlier-prone a distribution is or how heavy the tails of the distribution are and is defined as [25]

$$k = \frac{\frac{1}{N}\sum_{i=1}^{N}(X_i-\mu)^4}{\left(\frac{1}{N}\sum_{i=1}^{N}(X_i-\mu)^2\right)^2}. \quad (6)$$

Again, the kurtosis is an indication of how well the data follows a specific distribution by investigating the heaviness of the tails. The kurtosis of a Rayleigh distribution and a uniform distribution are 3.245 and 1.8, respectively. The kurtosis can therefore be used to determine whether the compression algorithm caused the data to deviate more from the applicable distribution compared to the uncompressed data.

- Entropy

The entropy, H, is a measure of the compressibility of the data or the randomness of the data and is defined as [25]

$$H = -\sum_{i=1}^{N} p(X_i)\cdot \log_2(p(X_i)) \quad (7)$$

where $p(X_i)$ is the probability of X_i occurring. A high entropy value means that the data are difficult to compress, while a lower value indicates that the data can easily be compressed to a smaller size. The entropy after compressing and decompressing the data should be similar to the entropy of the uncompressed data.

2.3. Data Histograms

The data histograms include the distributions of the in-phase (I), quadrature (Q), magnitude and phase components. By comparing the histograms before and after compression, the changes in the probability distribution caused by the compression algorithm can be visualised [10], [22].

2.4. Error Measures

In this subsection, the amplitude and phase distortions of the complex SAR data after decompression are investigated. In essence, the errors and distortions caused by the quantiser are being investigated here. Take note of the definition of the variables being used in this subsection: $g(x,y)$ is the pixels of the uncompressed data, $f(x,y)$ is the pixels of the decompressed data, and M and N are the number of rows and columns of the data, respectively.

- Mean Square Error (MSE)

The MSE is a measure of the performance of the quantiser and gives the total absolute encoding error between the uncompressed and decompressed data sets [6], [9], [22], [24]. It can be computed as

$$MSE = \frac{1}{MN}\sum_{x=1}^{M}\sum_{y=1}^{N}(g(x,y)-f(x,y))^2. \quad (8)$$

The MSE is computed using the magnitude components of the respective complex SAR data sets. The problem with using only the MSE to represent the distortion is that it depends strongly on the intensity scaling. Consequently, the MSE of different data sets can only be compared after the MSE values have been normalised. Therefore, the signal-to-quantisation-noise ratio is also evaluated in this study.

- Mean Phase Error (MPE)

In SAR processing, the phase information is used to focus the SAR image, and therefore, knowing the phase error after decompression gives an indication of the focusing error that will be present in the final image [22]. The MPE [6], [23], [24] is computed for the phase component of the data using the following equation

$$MPE = \frac{1}{MN}\sum_{x=1}^{M}\sum_{y=1}^{N}\left|\theta\big(g(x,y)\big)-\theta\big(f(x,y)\big)\right| \quad (9)$$

where θ is the phase component of the complex SAR data of both sets being evaluated.

- Signal-to-Quantisation-Noise Ratio (SQNR)

The SQNR an important parameter for image quality analysis since it is a measure of the signal-to-noise ratio after the compression and decompression of the data [19], [22]-[24]. It is used to measure the average amplitude distortion of the complex SAR data after compression and decompression have been implemented [6] and can be computed as

$$SQNR = 10\log_{10}\left[\frac{\sum_{x=1}^{M}\sum_{y=1}^{N}(g(x,y))^2}{\sum_{x=1}^{M}\sum_{y=1}^{N}(g(x,y)-f(x,y))^2}\right]. \quad (10)$$

The SQNR avoids the problem mentioned for the MSE by normalising the MSE. Therefore, both metrics are of use when investigating the quantisation effects.

3. Image-Domain Metrics

For conventional compression algorithms, the distortion is measured between the original and reconstructed data. However, for the compression of raw SAR data, the distortion is also measured in the image domain, after processing [13]. Thus, the distortion is measured between the SLC image of the uncompressed data and the SLC image of the decompressed data [13]. As previously discussed, only measuring distortion for the evaluation of compression algorithms for raw SAR data is not sufficient; since SAR has numerous outputs and applications that have different quality requirements. In most of the literature where compression algorithms for raw SAR data are evaluated, the only metrics used in this domain are the signal-to-distortion noise ratio

(SDNR) and/or the impulse response function (IRF) [6], [17]-[19], [27]. Although these are important metrics as they are strongly affected by compression algorithms, other metrics that evaluate factors other than visual quality should also be used to obtain a more complete quantification of the performance in a specific SAR application. The metrics that can be used to evaluate the effects of a compression algorithm in the image domain are described below. These metrics also provide better validation than the data-domain metrics since they evaluate the quality of the SAR Level 1 output. As can be seen from Fig. 1, this set of metrics is evaluated after processing the uncompressed data and the decompressed data to form the SLC SAR images that will be compared. The following metrics are suggested to evaluate the effects that compression algorithms introduce in the image domain.

3.1. Statistical Parameters

Higher order statistics can be used to characterise the distributions that the components of a data set follow. The statistical parameters of each data set are computed in the image domain to highlight the changes that occurred in the statistical characteristics of the SLC image [10], [12], [22]. Note that each metric is applied to the SAR image generated from the uncompressed data and the SAR image generated from the data after decompressing the compressed data to compare the results. For the equations of the metrics see (2) to (7) in Section 2. Also note that all statistical parameters, except the dynamic range, are computed using the magnitude and phase components of the complex image data. Note that the SLC image of the uncompressed data will act as the reference image for all comparisons.

- Dynamic Range

The dynamic range is computed using the magnitude component of the complex image data. There is a close correlation between the dynamic range and the contrast of the image; therefore, the change in this parameter can be compared to the change in the contrast ratio of the SAR images with and without compression. It should be noted that when the quality of an image is being evaluated, the dynamic range is generally seen as one of the image quality metrics. However, in this study it is evaluated as one of the statistical parameters to correspond with the statistical parameters of the data domain.

- Mean (First order statistic)

The compression algorithm should not drastically change the mean since the values are assumed to be quantized with only minor losses. The change in the mean should therefore be significantly smaller than the mean value of the uncompressed data. A change in the mean would introduce a bias in the final image, which would make the images more difficult to compare visually. However, if no clipping occurs (dynamic range is retained), the bias can be estimated and removed from the image. A large change in the mean would also indicate that the image exposure has been distorted by the compression algorithm, resulting in a loss of detail in the bright and/or dark regions of the image.

- Standard Deviation (Second order statistic)

Again, the compression algorithm is assumed to only quantize the data with minor losses. Therefore, the standard deviation of the image with the compression applied should be comparable with that of the image with no compression applied. A large change in the standard deviation would mean that the compression algorithm has increased the speckle content of the reference SAR image. Certain pixels are represented with a brighter or darker colour compared to the colour of the pixels in the reference image when the standard deviation changes. In this case the contrast of the SAR image will be affected.

- Skewness and Kurtosis (Third and Fourth order statistics)

These parameters can be used to determine how well the algorithm retains the statistical distribution of the SAR data and thus, how much statistical analysis on the SAR images generated from the decompressed data can be trusted.

- Entropy

The entropy is an indication of the information content of a SAR image. The entropy of the SAR image formed from the decompressed data should thus be similar to that of the SAR image formed from the uncompressed data, and can thus be used to verify this condition. A decrease in entropy would indicate that information has been lost, while an increase in entropy means that the compression algorithm has corrupted the reference image.

3.2. Image Quality Measures

Note that all the metrics in this subsection are computed for the SAR image formed from the uncompressed data, and for the SAR image formed from the decompressed data so that the results can be compared.

- Impulse Response Function (IRF)

A point target can be considered an impulse input to a SAR system. The point spread function (PSF) is equivalent to the IRF as a SAR system can be modelled as a two-dimensional linear system [28], [29]. Generally the PSF of an image is used to evaluate the performance or response of an imaging system like a SAR system [30], but in this case, the PSF or impulse response is used to determine the quality of a compression algorithm, as no other system changes are made. A good compression algorithm should not distort the IRF as this results in a loss of fidelity in the SAR images.

Illumination of a specifically designed scene is required to obtain the point target characteristics of a SAR system [31], [32]. The following elements are required within the scene:

1. point-like reflectors, and
2. reflectors positioned at the boundary between high and low backscatter areas.

Since only the data sets from the SAR system are available, the scene could not be set up with large point-like reflectors to measure the IRF. Although mission data generally have a scarcity of individual high signal-to-noise point targets in homogeneous areas of low reflectivity [32], [33], suitable geographical regions had to be identified from a real data set. See Section 5.1 for more information about the data set used.

The two metrics that are evaluated from the IPR are listed below [17]-[19]:

- 3 dB Impulse Response Width (IRW) in range and azimuth directions, which are related to the spatial resolutions. Spatial resolution (SR) is the ability of a system to distinguish two closely spaced point scatterers and can be computed as

$$SR = \frac{Number\ of\ pixels\ between\ the\ -3\ dB\ points}{\rho_{pixel}} \quad (11)$$

where ρ_{pixel} is the pixel size in the relevant direction [33].

- Peak-to-Side Lobe Ratio (PSLR) in the range and azimuth directions. PSLR provides an indication of whether the side lobe of a scatterer can mask an adjacent scatterer. It can be calculated as

$$PSLR = 20\log_{10}\left(\frac{IRF_{side}}{IRF_{main}}\right) \quad (12)$$

where IRF_{side} is the peak value of the first side lobe and IRF_{main} is the peak value of the main lobe of the IRF [33].

- Image Contrast (IC)

The image contrast is a metric to describe the quality of a SAR image [34], with a high image contrast ratio implying a crisp image and a low image contrast ratio suggesting a washed-out image [29]. IC is defined as the ratio of the average intensity of a distributed clutter background to the average intensity of a no-return background [29] and can be computed as [9],

$$CR = \frac{\sigma_{image}}{\mu_{image}}. \quad (13)$$

The dynamic range and the IC are related. However, both metrics are useful since the dynamic range only considers the single highest and single lowest values of the image, while the IC uses the mean and standard deviation, which are more representative of the variation of the dynamic range over the entire image.

- Global Contrast Factor (GCF)

GCF is a new approach in the field of image processing with applications in areas like rendering, tone mapping, volume visualization, and lighting design [34]. This metric has been added to the conventional metrics found in SAR literature, since it addresses the limitation of only using the darkest and brightest regions of an image to compute the IC. The GCF is indicative of the overall contrast of an image and is computed from the local contrast of an image at various resolutions [34]. Local contrast ratio is the contrast ratio of any small part of an image, and the GCF is defined as the weighted sum of the local contrasts of a range of smaller image sizes.

Human visual experiments can be used to construct a GCF computation procedure which is indicative of human image perception. SAR images are not always interpreted by human operators, so the weighting factors for human perception are not always relevant. Therefore, the method in [34] is adjusted to determine the GCF of the grayscale SAR images without applying the human perception adjustments. The steps below are followed.

1. Compute the linear luminance.

The linear luminance value for each pixel is computed by applying gamma correction to the image and scaling the result to be within the [0; 1] range. The linear luminance for the image is defined as

$$l = \left(\frac{k}{2^n - 1}\right)\gamma \quad (14)$$

where $\gamma = 2.2$ is the correction factor, $k \in \{0, 1, \ldots, 2^n - 1\}$ is the original pixel value, and n is the number of bits of the SAR image data.

2. Compute the local contrast.

The local contrast for pixel *i* is computed as the average magnitude of the difference between the pixel and its four neighbouring pixels,

$$lc_i = \frac{|l_i - l_{i-1}| + |l_i - l_{i+1}| + |l_i - l_{i-w}| + |l_i - l_{i+w}|}{4} \quad (15)$$

where the image has dimensions of $w \times h$. Note that for the corner pixels or pixels on the edges of the image, only the available neighbouring pixels are used in the computation.

3. Compute the average local contrast for the current resolution, *i*,

$$LC_i = \frac{1}{w \times h}\sum_{i=1}^{w \times h} lc_i. \quad (16)$$

Repeat step 1 to 3 for a number of resolutions of, for example [1, 2, 4, 8, …, 2^N] times the original resolution. A coarser image is obtained in each execution by taking the average of 4 pixels as the new pixel to halve the dimensions of the original image in both directions. This process continues until the coarsest resolution is reached. The number of chosen resolutions is defined as *N*.

4. Compute the global contrast factor as the average of the local contrasts for all resolutions. It is assumed that the system interpreting the SAR images is equally sensitive to changes at various frequencies and therefore, a weighting function is not required to compute the global contrast, in contrast to the requirements in [34].

$$GCF = \frac{1}{N}\sum_{i=1}^{N} LC_i. \quad (17)$$

An image with a high GCF is variation-rich, while an image with a low GCF appears uniform with less information [34].

3.3. Image Fidelity Measures

Image fidelity measures evaluate the level of exactness with which the original SAR image is reproduced. Therefore, these measures are an important measure of the quality of a compression algorithm. The different metrics are discussed below. Take note of the definition of the variables used in this subsection: $g(x, y)$ is the magnitude component of the uncompressed SLC image data, $f(x, y)$ is the magnitude component of the decompressed SLC image data, and M and N are the number of rows and columns of the image, respectively.

- Mean Square Error (MSE) and Mean Phase Error (MPE)

The MSE and MPE in this domain [13], [24] are both pixel by pixel measures of the change between the pixel values in the SAR image formed from the uncompressed data and the SAR image formed from the decompressed data. The MSE is computed for the magnitude component of the SAR images, while the MPE is computed for the phase component of the SAR images to measure the amplitude and phase distortions, respectively [6]. An important fact is that the MSE does not indicate whether the error is due to a large number of small errors, or whether it is due to a few large errors [22], [29]. It also depends strongly on the image intensity scaling. Therefore, the signal-to-distortion-noise ratio is also evaluated as part of this study. According to [29], the MSE is the most widely used image fidelity measure in SAR compression studies since it is mathematically and computationally simple to evaluate. To compute the MSE see (8) [9], [29]. The MPE can be computed using (9), where θ is the phase component of the two SLC images being compared.

- Signal-to-Distortion Noise Ratio (SDNR)

SDNR [6], [9], [17], [29] is a more global measure of the change and thus addresses the limitation mentioned for the MSE by normalising the MSE. It is also mathematically and computationally simple and therefore widely used in the literature [29]. To compute the SDNR see (10) [9], [29].

- Error Image

The error image [9], [22] can be computed as

$$e(x, y) = |g(x, y) - f(x, y)|. \quad (18)$$

The error image can be computed for the magnitude and phase components of the complex images in order to investigate both components. This metric can be used to visualise some of the corruptions that have occurred in the SAR images formed. It is important to note that many of the corruptions cannot be easily visualised by the human perceptual system and therefore, this metric is not able to fully represent the degradation that may have occurred.

4. SAR Technologies and Applications

The output or products of a SAR system can be used for various applications and each SAR technology renders different information. Although more than one SAR technology can be used for some of the applications, only a few of the well-known SAR technologies, with their primary applications, are discussed below. Since these technologies use different components of the SAR data, different metrics will be of importance for each technology when compression has to be implemented on board the platform. The important metrics for each technology are discussed below and also summarised in Table 1. It is important to note that all data-domain metrics are of importance for every SAR technology, thus emphasis will be placed on the image-domain metrics that need to be preserved in each case.

4.1. Single frequency, single polarisation SAR

Conventional SAR systems are used to create high resolution, two-dimensional images of the Earth's surface. Operation includes only a single pass over the scene using a single polarisation transmit/receive unit. The basic output is an image, for which the phase information is discarded [35]. Further processing can be performed to add radiometric and geometric corrections and/or speckle noise reduction to the image [36].

- Image classification

Image classification is identifying the different features within an image by distinguishing different levels of radar backscatter, e.g. high radar backscatter areas from medium, low or no return areas (NRAs) [2]. The different levels of return are used to identify groups of pixels with similar statistical properties and thus the image is divided in homogeneity categories [37]. The output is a detailed map of an entire region with its distinct features. Important applications of SAR image classification, where wide areas are being surveyed, are the mapping of land use (important for forestry and agriculture), assessment of the affected areas in disaster relief operations, and illegal or accidental oil spill detection [38]. For wide-area surveillance, automatic target recognition (ATR), also known as unsupervised algorithms, is increasingly being used, as it is a time-consuming process for a human operator to search through all the data [39]. The important metrics for these algorithms are the mean, variance and entropy of the SAR images, since these metrics are used to divide the image into homogeneity categories [37]. Furthermore, high image contrast is required for initial detection of areas of change within an image, so the IC and GCF are also important metrics for this application.

- Detection of man-made targets

When investigating the different levels of backscatter in a SAR image, man-made returns are highlighted since these objects provide a very high radar backscatter [1], [2]. The high levels of backscatter can be attributed to the characteristics of man-made objects which make them highly radar reflective. Although the detection of man-made targets is a very important military application, it is also required for earth observation applications. In military applications, SAR is used to detect and identify adversary facilities and assets of interest on the land and ocean, where counter-piracy and maritime law enforcement are important examples [40]. For

civilian applications, SAR images are not only used to detect ships in coastal regions, which aids in the monitoring of illegal fishing activities and vessel traffic, but they are also used to track urban and rural development over time [1], [38]. This application is mainly utilised in military systems and therefor requires good resolution and geometric accuracy [39]. When detecting and classifying man-made targets in military applications, it is important that the estimated location of the target corresponds to the real location with only a minimal margin of error. To ensure that the location is accurate, the IRF must be preserved. As part of the detection of targets, the magnitude or modulus of the SAR image is calculated [2] and the phase information is of less importance for the output. This means that the magnitude component should be preserved as well as possible when investigating the compression of the raw SAR data for man-made target detection. This condition can be monitored by comparing all the error measures of the magnitude component, which include the MSE and SDNR.

- Global monitoring (Change detection)

SAR is used for earth observation applications like ice monitoring and the study of climate change, where the global carbon cycle, the global energy/water cycle, and other human activities are monitored [38], [41]. The SAR system needs to be sensitive to small changes when monitoring a global cycle, consequently the radiometric resolution of the SAR system is an important factor [41]. The radiometric resolution of an imaging system describes its ability to detect very slight differences in reflected energy. In order to preserve the radiometric resolution of a system, frequent calibrations are required [41]. A high signal-to-noise ratio (SNR) indicates that the signal level is greater than the noise level and therefore the noise does not mask any of the small changes that may appear in a scene. The metrics of importance for this application are the MSE and the SDNR.

4.2. Ultra-wideband (UWB) SAR

UWB SAR has a very large bandwidth compared to conventional SAR systems [42]. The system uses short pulses with a rapid change in modulation, to produce a large bandwidth in the frequency domain. A very short pulse enables high resolution since the distances are measured more accurately [42]. The main advantages of UWB operation are improved resolution and more information about the reflectivity of the targets in the scene [42], [43].

- Imaging through unconventional mediums

The applications of UWB SAR include uses in the military and civilian domains. In the military domain UWB radar is used for foliage penetration, ground penetration, and through-wall detection [44], [45]. The ground penetration capabilities of UWB SAR make it highly affective for the detection of landmines [43]. Popular civilian applications include the monitoring of oil reservoirs [46], by imaging the perforations or fractures in the well, and medical imaging, like the detection of tumours [47]. The image quality depends strongly on the measurement accuracy and the dynamic range of the system [42]. For landmine detection, regions of interest are identified by measuring the amplitude difference between targets and the background noise [43]. To avoid a high number of false alarms, the noise in the system should be minimised. Therefore, dynamic range and SDNR are the metrics of importance and should be preserved when implementing a compression algorithm on board the platform.

Table 1 A summary of SAR technologies and their metrics of importance [19]

SAR Technology	**Primary Application**	**Main requirement**	**Important Metric(s)**
Single frequency, single polarisation SAR	Image classification	High image contrast	Statistical parameters, IC, GCF
	Detection of man-made targets	High sensitivity to point targets Magnitude component	Impulse response function: 3 dB IRW and PSLR IC, GCF,MSE
	Global monitoring	Noise should not mask changes	SDNR
Ultra-wideband SAR	Imaging through unconventional mediums	High radiometric resolution	SDNR
Interferometric SAR (InSAR)	Surface topography Measurement of displacements	Very high phase accuracy	Phase error: MPE and error image of phase
Polarimetric SAR (PolSAR)	Change detection and feature tracking	High phase accuracy	Phase error: MPE and error image of phase

4.3. Interferometric SAR (InSAR)

InSAR uses the phase difference between two SAR images acquired at two distinct times or from slightly different positions to measure changes to a specific surface [35], [39], [48]. Since the phase of each pixel contains range information that is accurate to a fraction of the radar wavelength, it is possible to detect and measure miniscule path length differences, velocities, and height differences with very high accuracy [7], [39], [48].

- Surface topography

Topographic maps or three-dimensional models, known as digital elevation models (DEMs), can be constructed using InSAR since the height variations can accurately be measured [35]. These maps are used to analyse the surface parameters, for modelling and simulation in various fields, and to create accurate maps, to mention only a few uses.

- Measurement of displacements

InSAR is typically used for various remote sensing applications like the measurement of displacements. These include the detection of moving objects (for example cars or ships), and geophysical applications like monitoring earthquakes, landslides, glaciers, and volcanoes [2], [38], [49]. The changes in the surface are detected by comparing two InSAR topographic maps produced before and after a natural event occurred [35].

Since the phase difference is used to detect small differences, it is therefore evident that preserving the phase content is important for this technology. The metrics of importance include the MPE and the error image of the phase component as it can provide a visual representation of the error between two SAR images.

4.4. Polarimetric SAR (PolSAR)

PolSAR is an advanced imaging technique where the radar transmits and receives multiple polarisations [35]. Since the full scattering matrix is measured, the system is sensitive to the shape, orientation and dielectric properties of the scatterers, which means much more information is obtained than with conventional, single polarisation SAR systems [35], [48].

- Change detection and feature tracking

PolSAR has many applications including agriculture (soil moisture extraction and crop assessment), oceanography, forestry (forest monitoring, classification, and tree height estimation), and disaster monitoring (oil spill detection, disaster assessment) [35], [48], [50]. For these applications, the phase information of the SAR image is required [2], so it is important that the phase information be preserved when compressing the raw data. The metrics of importance include the MPE and the error image of the phase component as a visual representation of the error between two SAR images.

5. Results

In this section, the metrics that were discussed in Sections 2 and 3 will be applied to evaluate the performance of SAR compression algorithms. The three algorithms that were implemented to illustrate how the metrics can be applied are the block adaptive quantiser (BAQ), fast Fourier transform BAQ (FFT-BAQ) and the flexible dynamic BAQ (FDBAQ). These algorithms are found to be best suited for the compression of raw SAR data in a processing and cost constrained environment due to their simplicity, reliability and their current use as the basis method of evolved compression methods used in SAR sensor systems [7], [8], [11], [19]. Implementing these algorithms represents compression in the time and frequency domains. The performance of these algorithms was evaluated by implementing the process described in Fig. 1.

In a SAR system the decompression and SAR processing are performed at a ground station after the compressed data have been transmitted from the platform or read from platform data storage.

Note that the compression ratio and processing parameters were kept constant in order to ensure a fair comparison. For example, the same SAR signal processor was used for all data sets, and the metrics were computed using the same equations and at the same stage of the process, with the compression algorithms being the only varying factor.

5.1. Data Sets used

The data sets that were required for this study are of the type: Level 0 data. Data produced by SAR systems are classified as Level 0, Level 1 and Level 2 to distinguish the amount of processing which has been performed on the data [36]. Level 0 SAR products contain the raw SAR data, before any processing. Level 0 products are divided into four product types but only the SAR Level 0 standard products, which are the received echoes, were required for this investigation.

Data aggregation was not executed; the data sets were provided by the Radar Imaging and Fusion Research Group of the Council for Scientific and Industrial Research (CSIR). The CSIR data sets include three SAR data sets of different scenes.

The specifications of the CSIR SAR system used to gather the real SAR data are: C-band operation and a down-

Table 2 CSIR data sets characteristics

Parameter	Specification
Platform	Airborne
Operating Mode	Stripmap
Frequency Band	C-band
RF Bandwidth	200 MHz
Polarisation	Linear Vertical
Transmission	Pulsed
Quantisation	8-bit I, 8-bit Q
Scenes	Rural, Mine Setting, Sub-urban

range resolution of 1 m. The flightpath for the SAR mission covered areas in and around Pretoria, South Africa, and the mission took place in June, 2017. Thus, the data represent different terrains which include residential, natural and agricultural areas (low-urban and mid-urban data). Different terrains represent different reflectivity and in essence different distributions [51]. This must be taken into account when choosing the compression algorithm to ensure its effectiveness. The characteristics of the data sets are summarised in Table 2.

5.2. Data-Domain Metrics Results

The metrics discussed in Section 2 are evaluated and the results are summarised below. All three of the available data sets were evaluated for both compression methods with similar tendencies being observed. Only the results for the sub urban scene, where a residential area next to a dam was illuminated, are considered in this section since the data sets show similar tendencies, and thus one data set is representative of all data sets.

In Table 3, the results of the statistical parameters are summarised. There is about a 74 dB difference between the dynamic range of the results obtained using the FDBAQ or BAQ methods, and the FFT-BAQ method. The dynamic range after applying the FFT-BAQ method are also much greater than the dynamic range of the uncompressed data set. The reason for the FFT-BAQ result could be because the compression takes place in the frequency domain while the metrics are computed in the time domain. Since the dynamic range is computed by only considering the smallest and largest values of the data set, a very small minimum value caused by the compression in the frequency domain has a very large effect on the dynamic range, measured in the time domain.

When considering all other statistical parameters, all the methods perform well as the values differ only slightly from the original, uncompressed values. The skewness and kurtosis are two metrics that are of importance since they are representative of the deviation of the distributions of the magnitude and phase components from the original distributions. The results show that the FFT-BAQ method causes minimal deviation from the original distributions. For a Rayleigh distribution the skewness should be close to 0.63, while the kurtosis should have a value of 3.245. The results show that even after applying the compression algorithms, each component can still be assumed to follow the same distribution as the original, uncompressed data set. In Fig. 4, found in the Appendices, the variation of the statistical parameters of the data due to the BAQ method is represented visually by the histograms of each component before and after the compression. The effect of the compression in the time domain, as is a characteristic of the BAQ method, can be seen by only certain values being represented. In Fig. 5, the distributions for each component before and after applying the FFT-BAQ method are represented. It can be seen that the data, after applying the algorithm, closely follow the original distribution since the compression was performed in the frequency domain and, thus, the quantisation effect is spread across time domain values. Finally, applying the FFT-BAQ method, results in all possible values still being represented in the time domain. In Fig. 6, the distributions for each component before and after applying the FDBAQ method are represented. The operation of the FDBAQ method can be visualised as it can be seen that the values represented after decoding are highly variable, since the BAQ was applied for more than one output bit rate. The results show that the data histograms are an important visual aid in determining the

Table 3 Statistical parameters of the sub urban data set in the data domain

Metric	Uncompressed Value	Value after BAQ method	Value after FFT-BAQ method	Value after FDBAQ method
Compression Ratio	-	4	4	4
Dynamic Range	30 892	9.5313	41 525	7.9716
Mean (mag)	11.5280	12.5146	9.3734	10.7012
Mean (phase)	0.0227	0.0224	0.0039	0.2705
Standard deviation (mag)	7.2394	6.9086	6.1662	6.5931
Standard deviation (phase)	1.8218	1.7927	1.8160	1.7178
Skewness (mag)	1.1248	0.7381	1.2591	0.6226
Skewness (phase)	-0.0196	-0.0190	-0.0039	0.0271
Kurtosis (mag)	4.5765	2.7022	4.9922	3.3574
Kurtosis (phase)	1.7917	1.7207	1.7965	1.9783
Entropy (mag)	6.4452	7.3038	6.2750	6.6900
Entropy (phase)	7.9996	3.4214	8.0000	3.8848

Table 5 Error measures for the sub urban data set in the data domain

Metric	Value after BAQ method	Value after FFT-BAQ method	Value after FDBAQ method
MSE	15.8893	29.7778	14.6120
SQNR	10.67dB	7.94dB	11.03dB
MPE	0.2502	0.9690	0.5896

effects of a compression algorithm on the raw SAR data in the data domain.

The error measures are summarised in Table 5. The FFT-BAQ method achieves the worst results for the error measures. These results can be attributed to the variable compression ratio of the code scheme used in the FFT-BAQ method. The code scheme encodes a portion of the data that has the lowest amount of energy in the frequency domain with 0 bits, whereas the high energy frequency components are encoded with 2 or 3 bits. Encoding data with 0 bits represents a loss of information, which is in the data domain and has an effect on the MSE and the SQNR. Due to the nature of operation of the FFT, an error is introduced to each element in the set, which is then used in the computation of these metrics. It is thus evident that these metrics are used to determine the effects of the quantisation for each method in the data domain, which will differ from the effects they have in the image domain as will be seen in the next subsection. From the phase error metrics, it seems that the BAQ method has a smaller effect on the phase in the data domain than the FFT-BAQ and FDBAQ methods. However, when considering the entropy (Table 3) of the data it can be seen that the data have higher information content when the FFT-BAQ method is applied. There is a relatively large difference between the phase entropy of the FFT-BAQ method and that of the two time domain methods. This shows that the time domain methods have a detrimental effect on the phase information content of the data in the data domain. Therefore, for an application where phase information in the data domain is of importance, the method which better preserves the phase (the FFT-BAQ method in this case) would be preferred.

After investigating the results in this domain, it was seen that some metrics favoured the time domain methods, while some metrics favoured the frequency domain method. Therefore, a decision on the performance of a raw SAR data compression algorithm cannot be made by only considering the metrics in the data domain. The metrics in the image domain also need to be considered when choosing a suitable algorithm for an application.

5.3. Image-Domain Metrics Results

The metrics discussed in Section 3 are evaluated and the results are summarised below. The same metrics were evaluated for all three compression methods and for the same data set. These metrics are evaluated in the image domain which means they are evaluated after the SAR processing was implemented. The SAR processing method used for the CSIR data sets is a modified 1D time domain algorithm.

In Table 4 the results of the statistical parameters of the sub urban data set are summarised. The statistical parameters for each method suggest that all methods perform equally well in this domain as the statistical characteristics of the original SAR image did not change significantly after applying any of the compression algorithms. However, the one metric that shows a greater difference between the three methods, is the dynamic range. In the data domain, there was a 74 dB difference between the dynamic ranges of the time domain methods and the frequency domain method. However, in the image domain, the dynamic range of the FDBAQ method is about 6 dB greater than that of the FFT-BAQ method. This shows that the coherent SAR processing exploits averaging to reduce the effects caused by the quantisation in the data domain, so that great differences in the data domain have little effect in the image domain.

Table 4 Statistical parameters of the sub urban data set in the image domain

Metric	Uncompressed Value	After BAQ method	After FFT-BAQ method	After FDBAQ method
Dynamic Range	5.75×10^{5}	3.52×10^{5}	9.02×10^{5}	1.78×10^{6}
Mean (mag)	5692.2	6274.4	5634.3	5516.2
Mean (phase)	2.51×10^{-5}	1.02×10^{-4}	1.68×10^{-4}	-2.43×10^{-4}
Standard deviation (mag)	5571.7	5695.7	5517.4	5119.5
Standard deviation (phase)	1.8138	1.8138	1.8139	1.8138
Skewness (mag)	19.2464	19.0617	18.0450	18.9089
Skewness (phase)	7.97×10^{-5}	-6.52×10^{-5}	-7.91×10^{-5}	1.03×10^{-4}
Kurtosis (mag)	1345.9	1326.1	1170.3	1299.7
Kurtosis (phase)	1.7998	1.8	1.8002	1.7999
Entropy (mag)	2.2491	2.3297	2.3426	2.3224
Entropy (phase)	8	8	8	8

Table 7 Image fidelity measures for the sub urban data set

Metric	Value after BAQ method	Value after FFT-BAQ method	Value after FDBAQ method
SDNR	11.42dB	14.30dB	12.51dB
MSE	4.58×10^6	2.36×10^6	3.56×10^6
MPE	1.5695	1.5462	1.5656

After SAR processing, the SAR image is produced and the visual quality of the image can be determined by the image quality measurements. These metrics include the impulse response function (IRF) and the image contrast and are summarised in Table 6. When considering the image contrast ratio, which directly relates to the dynamic range, it can be seen that the SAR image after applying the FFT-BAQ method has the highest contrast ratio. This result can also be confirmed visually, since a higher contrast ratio means a crisper image. When comparing Fig.2b, Fig.2c and Fig.2d, a slightly higher level of crispness of the SAR image after the FFT-BAQ method can be seen. The boundaries in the image between, for example, the water of the dam and the residential area, can be distinguished more easily for the image with FFT-BAQ applied. Quantising the data in the frequency domain causes less image degradation than quantising the data in the time domain. It has a visible effect on the dynamic range and the contrast ratio of the SAR images, which are slightly higher when the FFT-BAQ method is applied.

Another important image quality metric is the IRF of the SAR system. It is the response of the SAR system to a point scatterer. For this investigation the sub-urban scene data set was used since the scene contained more bright scatterers than the rural or mine scenes. Usually the IRF of a SAR system is determined by placing targets with a known RCS, like a transponder or reflector, in the scene to measure the response. However, for the data sets available for this study, a target of opportunity had to be used. Thus, the method explained in [52] was executed and the extracted target can be seen in Fig.3a. The IRF was determined for the case where no compression algorithm was applied to the data to serve as the reference as well as for the case where compression was applied. The effect that each compression algorithm has on the impulse response can then be determined. In Table 6 the IRF results are summarised. The IRF in the range and cross-range directions are plotted in Fig.3b and Fig.3c. The 3 dB widths after applying the respective compression methods correspond well to the reference values. Although the side lobes are higher in the range direction, for all three compression methods, the overall shape of the reference IRF is maintained. Therefore, none of the compression methods has a detrimental effect on the impulse response of the original SAR image without any compression applied. If the goal of the SAR mission was to identify man-made targets, the compression algorithm with the smallest effect on the IRF would be preferred. Since man-made targets have similar scattering characteristics to point scatterers, the impulse response of the system needs to be preserved.

The image fidelity measures are an indication of the exactness with which the SAR image, with compression applied, was reproduced compared to the reference SAR image. The results are given in Table 7. It can be seen that the FFT-BAQ method has the smallest errors in this domain, since the SDNR is the highest, while the MSE and MPE are smaller than for the two time-domain methods.

After investigating the results in the image domain it is clear that the quality of the SAR images after applying the FFT-BAQ method is better than the quality of the SAR images after applying the BAQ or FDBAQ methods. For all three methods, the characteristics of the scene can easily be identified, but the image is crisper after applying the FFT-BAQ method.

5.4. Computational Complexity

Although certain conclusions can be made about which algorithm would be best for a certain application based on the metrics, another factor is the computational complexity. An algorithm may perform very well in terms of reduction rate and also cause the least degradation of the final product, but being an order of magnitude more complex than another method may be the one reason the algorithm is not feasible to implement in a system. Therefore, the computational complexity of the three compression algorithms applied in this paper, will be investigated and compared. Big O notation will be used to describe the complexity of the encoding steps of each algorithm in a simplified manner. Only the complexity of the encoding operations is considered since the encoding will take place on board the SAR platform where SWAP-C limitations apply, while the decoding operations will be performed at the ground station.

5.4.1. Computational complexity of the BAQ method:

Compression Steps	Complexity
1. Split data into I & Q components	O(1)

Table 6 Image Quality Measures for the sub urban data set

Metric	Original Value	After BAQ method	After FFT-BAQ method	After FDBAQ method
IRW (range)	0.9994 m	0.9369 m	0.9994 m	0.9369 m
IRW (azimuth)	9.7438 m	9.7438 m	9.8062 m	9.7438 m
PSLR (range)	-17.02 dB	-10.75 dB	-10.51 dB	-10.63 dB
PSLR (azimuth)	-23.59 dB	-27.43 dB	-24.79 dB	-25.22 dB
Image Contrast	0.9788	0.9078	0.9793	0.9281
Global Contrast Factor	0.0955	0.0927	0.0940	0.0919

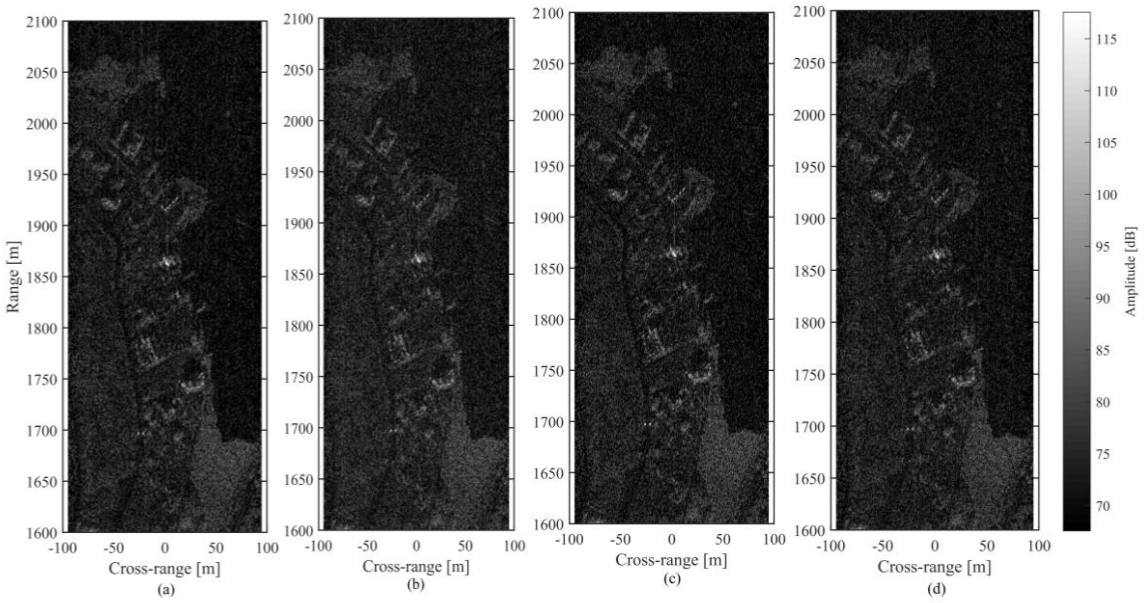

Fig.2. *SAR images after SAR processing. (a) SAR image of the uncompressed data. (b) SAR image after the BAQ method. (c) SAR image after the FFT-BAQ method. (d) SAR image after the FDBAQ method*

2. Break data into [200×200] blocks	O(1)
3. Calculate the σ of each bock	O(4N + 3)
4. Encode the data	O(N)

The complexity of the encoding part of the BAQ method can be computed as below,

$$O(BAQ) = O(1 + 1 + 4N + 3 + N) \quad (19)$$
$$= O(5N + 5) \quad (20)$$
$$\approx O(5N) \quad (21)$$
$$\approx O(N) \quad (22)$$

where *N* is the number of elements in the data set.

Therefore, the computational complexity of the BAQ method is a linear function of the number of elements in the data set which relates to the volume of data.

5.4.2. Computational complexity of the FFT-BAQ method:

Compression Steps	**Complexity**
1. Split data into I & Q components	O(1)
2. Break data into [200×200] blocks	O(1)
3. Calculate the σ_1 of each bock	O(4N + 3)
4. Normalise the data by σ_1	O(N)
5. Break data into [1024×1024] blocks	O(1)
6. Perform 2D FFT on each block	O(K(LMlog(LM))
7. Break data into [200×200] blocks	O(1)
8. Calculate the σ_2 of each bock	O(4N + 3)
9. Encode the data	O(N)

The complexity of the encoding part of the FFT-BAQ method can be computed as below,

$$O(FFT - BAQ) = O(10N + 10 + K(LM \log LM)) \quad (23)$$
$$\approx O(N + K(LM \log LM)) \quad (24)$$
$$\approx O\left(N + \frac{N}{LM}(LM \log LM)\right) \quad (25)$$
$$\approx O(N + N \log LM) \quad (26)$$
$$\approx O(N + N \log \frac{N}{K}) \quad (27)$$
$$\approx O(N + N \log N) \quad (28)$$

where *N* is the number of elements in the data set, *M* is the number of rows in each FFT block, *L* is the number of columns in each FFT block and *K* is the number of blocks to perform the 2D FFT on, thus $K = \frac{N}{LM}$.

Therefore, it can be seen that the computational complexity of the FFT-BAQ method is a logarithmic function of the number of elements in the data set which relates to the volume of data.

5.4.3. Computational complexity of the FDBAQ method:

Compression Steps	**Complexity**
1. Split data into I & Q components	O(1)
2. Break data into [200×200] blocks	O(1)
3. Calculate the signal power and noise power of each bock	O(4N + 3)
4. Select bit rate for encoding	O(P)
5. Encode the data	O(N)

The complexity of the encoding part of the FDBAQ method can be computed as below,

$$O(BAQ) = O(1 + 1 + 4N + 3 + P + N) \quad (29)$$
$$= O(5N + P + 5) \quad (30)$$
$$\approx O(5N) \quad (31)$$
$$\approx O(N) \quad (32)$$

where *N* is the number of elements in the data set and *P* is the number of blocks that the data set is split into.

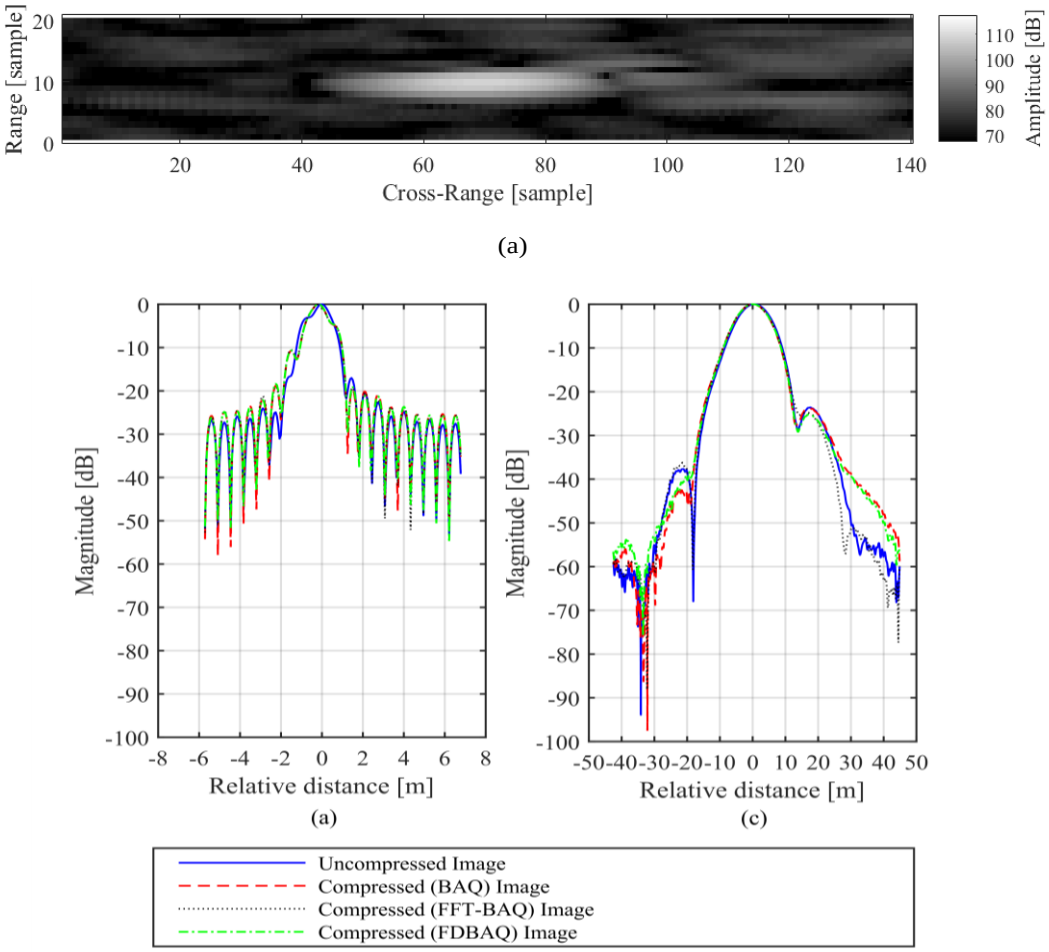

Fig.3. *IRF after no compression, after the BAQ method and the FFT-BAQ method. (a) Extracted target. (b) Range direction. (c) Cross-range direction.*

Therefore, the computational complexity of the FDBAQ method is a linear function of the number of elements in the data set which relates to the volume of data.

6. Conclusion

For some SAR applications a certain level of degradation is acceptable and the outcome of the SAR mission will be unaltered. For other applications much less degradation can be tolerated as it will heavily affect the outcome of the mission. It could also be that for a certain application, one component of the data is more important to preserve than another.

The metrics applied in the two different domains can be used to determine the effects of compressing the raw SAR data. Firstly, the compression algorithm metrics can be evaluated to determine the effects of the compression algorithm in the data domain. Important metrics include the compression ratio, the entropy, statistical parameters like the skewness and kurtosis to measure the deviation from the original distributions of the uncompressed data, and the dynamic range. The data histograms are an important visual representation of the effects of the compression algorithm on the data. An important error measure in the data domain is the SQNR and the phase error measures for applications where phase information is an integral part of forming the output of the SAR system.

After the SAR processing another set of metrics can be evaluated to determine the degradation in the image domain. Here, the emphasis is on the quality of the SAR image that was produced from the data that had undergone the compression on board the SAR platform. Important metrics in the image domain include the dynamic range, the entropy, the IRF, the contrast ratio, as well as the error measure, SDNR. In the image domain, the phase error measures, for example the phase MSE, are important for applications where phase information is an integral part of forming the output of the SAR system. The SAR technologies where the phase information is the most important component of the complex SAR image, is InSAR and PolSAR.

Although a compression algorithm may have performed better than another in one or both domains, the computational complexity is of importance when practical implementation needs to be considered. Therefore, the computational complexity of each algorithm was determined using big O notation. Due to the SWAP-C limitations of modern SAR platforms, the trade-off between the computational complexity and the performance of the compression algorithm is a very important consideration. Depending on the application of the SAR system, one or the other will be of higher priority.

The metrics proposed in this paper can be used during the design phase of a SAR system, when a compression algorithm for implementation on board a platform needs to be chosen. The results of the metrics can be used to conduct a

thorough investigation on the performance and complexity of different compression algorithms for raw SAR data.

7. Acknowledgements

The authors would like to thank the handing Associate Editor and the anonymous reviewers for their valuable comments and suggestions for this paper.

This work was supported by the CSIR and the Department of Science and Technology (DST) whom also supplied the necessary data sets to conduct the study. The financial assistance of the South African DST towards this research is hereby acknowledged. Opinions expressed and conclusions arrived at, are those of the authors and are not necessarily to be attributed to DST.

This work is based on the research supported in part by the National Research Foundation of South Africa (NRF) (Grant specific unique reference number (UID) 85845). The NRF Grant holder acknowledges that opinions, findings and conclusions or recommendations expressed in any publication generated by the NRF supported research are that of the author(s), and that the NRF accepts no liability whatsoever in this regard.

A special thanks to Jani Steyn, a signal analyst at the CSIR who was responsible for the SAR processing of the data.

8. References

[1] Richards, M. A., Scheer, J. A., Holm, W. A.: 'Principles of Modern Radar, Volume I - Basic Principles' (SciTech Publishing, Raleigh, NC, 2010)

[2] Moreira, A.: 'Synthetic Aperture Radar (SAR): Principles and Applications'. 4th Advanced Training Course in Land Remote Sens., Athens, Greece, July 2013, pp. 1-62 Available: https://earth.esa.int/documents/10174/642943/6-LTC2013-SAR-Moreira.pdf.

[3] McHale, J. (2011, April 21): 'TRACER synthetic aperture radar from Lockheed Martin completes testing aboard Predator UAV', http://www.avionics-intelligence.com/articles/2011/04/tracer-synthetic-aperture.html, accessed 1 October 2016

[4] Keller, J. (2014, October 15): 'Army researchers choose IMSAR to develop small radar systems for unmanned aerial vehicles', http://www.militaryaerospace.com/articles/print/volume-25/issue-10/unmanned-vehicles/army-researchers-choose-imsar-to-develop-small-radar-systems-for-unmanned-aerial-vehicles.html, accessed 1 October 2016

[5] Belward, A. S., Skøien, J. O.: 'Who launched what, when and why; trends in global land-cover observation capacity from civilian earth observation satellites', ISPRS J. Photogramm. Remote Sensing, 2015, 103, pp. 115-128

[6] Liu, J., Zhou, Q.: 'SAR raw data compression based on geometric characteristic of gaussian curve', 7th Int. Conf. Digit. Image Process. (ICDIP), Los Angeles, USA, 2015, pp. 1-7

[7] Guccione, P., Belotti, M., Giudici, D., Guarnieri, A. M., Navas-Traver, I.: 'Sentinel-1A: Analysis of FDBAQ Performance on Real Data', IEEE Trans. Geosci. Remote Sens., 2015, 53, (12), pp. 6804-6812

[8] Kwok, R., Johnson, W. T. K.: 'Block Adaptive Quantization of Magellan SAR Data', IEEE Trans. Geosci. Remote Sens.(GRS), 1989, 27, (4), pp. 375-383

[9] Parkes, S. M., Clifton, H. L.: 'The compression of raw SAR and SAR image data', Int. J. Remote Sens., 1999, 20, (18), pp. 3563-3581

[10] Kuduvalli, G., Dutkiewicz, M., Cumming, I.: 'Synthetic aperture radar signal data compression using block adaptive quantization'. Science Information Management and Data Compression Workshop, Greenbelt, MD, USA, 1994, Available: https://ntrs.nasa.gov/search.jsp?R=19950008176

[11] Fischer, J., Benz, U., Moreira, A.: 'Efficient SAR raw data compression in frequency domain'. Int. Geosci. Remote Sens. Symp. (IGARSS), Hamburg, Germany, February 1999, pp. 2261-2263

[12] Morin, X., Barba, D., El Assad, S.: 'Vector quantization of raw polarimetric SAR data by using their statistical properties'. Proc. SPIE. 3217, Image Processing, Signal Processing, and Synthetic Aperture Radar for Remote Sensing, December 1997, London, United Kingdom, pp. 124-131

[13] Rane, S., Boufounos, P., Vetro, A., Yu, O.: 'Low complexity efficient raw SAR data compression'. Proc. SPIE. 8051, Algorithms for Synthetic Aperture Radar Imagery XVIII, April 2011, Orlando, Florida, United States, pp. 1-11

[14] Ikuma, T., Naraghi-Pour, M., Lewis, T.: 'Predictive Quantization of Range-Focused SAR Raw Data', IEEE Trans. Geosci. Remote Sens.(GRS), 2012, 50, (4), pp. 1340-1348

[15] Boustani, A. E., Brunham, K., Kinsner, W.: 'An optimal wavelet for raw SAR data compression'. Can. Conf. Electr. Comput. Eng., Montréal, Canada, May 2003, pp. 2071-2074

[16] Wang, M.: 'Raw SAR data compression by structurally random matrix based compressive sampling'.2nd Asian-Pacific Conf. on Synthetic Aperture Radar, Xian, Shanxi, China, October 2009, pp. 1119-1122

[17] Magli, E., Olmo, G.: 'Lossy Predictive Coding of SAR Raw Data', IEEE Trans. Geosci. Remote Sens. (GRS), 2003, 41, (5), pp. 977-987

[18] Moreira, A., Blaeser, F.: 'Fusion of block adaptive and vector quantizer for efficient SAR data compression'. Int. Geosci. Remote Sens. Symp. (IGARSS), Tokyo, Japan, August 1993, pp. 1583-1585

[19] Benz, U., Strodl, K., Moreira, A.: 'A Comparison of Several Algorithms for SAR Raw Data Compression', IEEE Trans. Geosci. Remote Sens. (GRS), 1995, 33, (5), pp. 1266-1276

[20] Max, J.: 'Quantizing for minimum distortion', IRE Trans. on Information Theory, 1960, 6, (1), pp. 7-12

[21] Lloyd, S. P.: 'Least squares quantization in PCM', IEEE Trans. on Information Theory, 1982, 28, (2), pp. 129-137

[22] Dutkiewicz, M., Cumming, I.: 'Methods of evaluating the effects of coding on SAR data'. The Space and Earth Science Data Compression Workshop, NASA, Goddard Space Flight Center, January 1993, pp. 59-72

[23] Qi, H.-M., Yu, W.-D., Yuan, X.-Z., Guo, Z.-Y., Tian, X.-W.: 'Performance evaluation of amplitude-phase algorithm for SAR raw data compression'. International Geoscience and Remote Sensing Symposium (IGARSS), Denver, CO, USA, 2006, pp. 809-812

[24] Agrawal, N., Venugopalan, K.: 'Analysis of complex SAR raw data compression'. Prog. Electromagn. Research Symp. (PIERS), Cambridge, Massachusetts, July 2008, pp. 141-146

[25] Bulmer, M. G.: 'Principles of Statistics' (Dover Publications Incorporated, New York, 1979)

[26] Archer, C. O.: 'Some properties of Rayleigh distributed random variables and of their sums and products'. Naval Missile Center, Point Mugu, California, Tech. Rep. TM-67-15, April 1967

[27] Naraghi-Pour, M., Cortez, R., Ikuma, T.: 'Analysis-by-synthesis compression of range-focused SAR raw data'. IEEE Trans. Aerosp. Electron. Syst., 2015, 51, (2), pp. 1298-1309

[28] Sullivan, R. J.: 'Radar Foundations for Imaging and Advanced Concepts' (SciTech Publishing, Raleigh, North Carolina, 2004)

[29] Penrod, T. D., Kuperman, G. G.: 'Image quality analysis of compressed synthetic aperture radar imagery', U.S. Air force, Tech. Rep. AL/CF-TR-1993-0156, Jan. 1993

[30] Raney, R. K.: 'Theory and Measure of Certain Image Norms in SAR', IEEE Trans. Geosci. Remote Sens., 1985, GE-23, (3), pp. 343-348

[31] Mitchel, R. H., Marder, S.: 'Synthetic Aperture Radar (SAR) Image Quality Considerations', Optical Eng., 1982, 21, (1), pp. 048-055

[32] Clinard, M. S., Farnung, C. E., Kopacz, P., et al.: 'Impulse response function (IPR) estimation method using detected synthetic aperture radar (SAR) mission data'. Proc. SPIE 4727, Algorithms for Synthetic Aperture Radar Imagery IX, Orlando, Florida, United States, August 2002, pp. 178-185

[33] Zhang, H., Li, Y., Su, Y.: 'SAR image quality assessment using coherent correlation function'. 5th Int. Congr. Image Signal Process. (CISP), Chongqing, China, October 2012, pp. 1129-1133

[34] Krešimir, M., Neumann, L., Neumann, A., Psik, T., Purgathofer, W.: 'Global contrast factor - a new approach to image contrast'. Comput. Aesthetics Graph., Vis. Imag., Girona, Spain, 2005, pp. 159-167

[35] Stimson, G. W., Griffiths, H. D., Baker, C. J., Adamy, D.: 'Stimson's Introduction to Airborne Radar' (SciTech Publishing, Edison, New Jersey, 2014, 3rd ed.)

[36] Curlander, J. C., McDonough, R. N.: 'Synthetic Aperture Radar Systems and Signal Processing' (John Wiley and Sons, New York, 1991)

[37] Solberg, A. H. S., Brekke, C., Husoy, P. O.: 'Oil Spill Detection in Radarsat and Envisat SAR Images', IEEE Trans. Geosci. Remote Sens. (GRS), 2007, 45, (3), pp. 746-755

[38] Inggs, M. R., Lord, R. T.: 'Applications of satellite imaging radar'. South African Institute of Electrical Engineers (SAIEE), South Africa, 2000, pp. 1-8

[39] Oliver, C., Quegan, S.: 'Understanding Synthetic Aperture Radar Images' (SciTech Publishing, Raleigh, North Carolina, 2004)

[40] Greidanus, H., Alvarez, M., Cokacar, T., Pesaresi, A., Santamaria, C., Kyovtorov, V.: 'Satellite SAR ship detections from PMAR in support of Cutlass Express' (European Union, Luxembourg, Tech. Rep. LB-NA-25140-EN-N, 2011)

[41] Lin, C. C. Mancini, P. L.: 'A SAR instrument for global monitoring of land surfaces and polar ice'. Int. Geosci. Remote Sens. Symp. (IGARSS), Pasadena, California, August 1994, pp. 1525-1528

[42] Zwick, T., Wiesbeck, W., Timmermann, J., Adamiuk, G.: 'Ultra-Wideband RF System Engineering' (Cambridge University Press, Cambridge, United Kingdom, 2013)

[43] Fu-lai, L., Qian, S., Yu-ming, W., Han-hua, Z., Zhi-min, Z.: 'Ultra-wideband synthetic aperture radar landmine detection based on landmine-enhanced imaging'. IEEE International Conference on Ultra-Wideband (ICUWB), Sydney, NSW, Australia, September 2013, pp. 201-204

[44] Ren, Y. J., Lai, C. P., Chen, P. H., Narayanan, R. M: 'Compact Ultra-wideband UHF Array Antenna for Through-Wall Radar Applications', IEEE Antennas and Wireless Propagation Letters, 2009, 8, pp. 1302-1305

[45] Naveena, M., Singh, D. K., Singh, H.: 'Design of UHF band UWB antenna for foliage penetration application'. IEEE International Conference on Antenna Innovations Modern Technologies for Ground, Aircraft and Satellite Applications (iAIM), Bangalore, India, 2017, pp. 1-3

[46] Oloumi, D., Pettersson, M. I., Mousavi, P., Rambabu, K.: 'Imaging of Oil-Well Perforations Using UWB Synthetic Aperture Radar', IEEE Trans. Geosci. Remote Sens., 2015, 53, (8), pp. 4510-4520

[47] Oloumi, D., Boulanger, P., Kordzadeh, A., Rambabu, K.: 'Breast tumor detection using UWB circular-SAR tomographic microwave imaging'. 37th Annual International Conference of the IEEE Engineering in Medicine and Biology Society (EMBC), Milan, Italy, August 2015, pp. 7063-7066

[48] Moreira, A., Prats-Iraola, P., Younis, M., et al.: 'A Tutorial on Synthetic Aperture Radar', IEEE Geosci. Remote Sens. Mag., 2013, 1, pp. 6-43

[49] Massonnet, D., Feigl, K. L.: 'Radar Interferometry and its Application to Changes in the Earth's Surface', Rev. Geophys., 1998, 36, (4), pp. 441-500

[50] van Zyl, J., Kim, Y.: 'Synthetic Aperture Radar Polarimetry' (John Wiley and Sons, Hoboken, New Jersey, 2011)

[51] Long, M. W.: 'Radar Reflectivity of Land and Sea' (Artech House, Boston, 2001, 3rd edn.)

[52] Martinez, A., Marchand, J.: 'SAR Image Quality Assessment', Spanish J. Remote Sens. (RAET), 1993, 2, pp. 1-7

9. Appendices

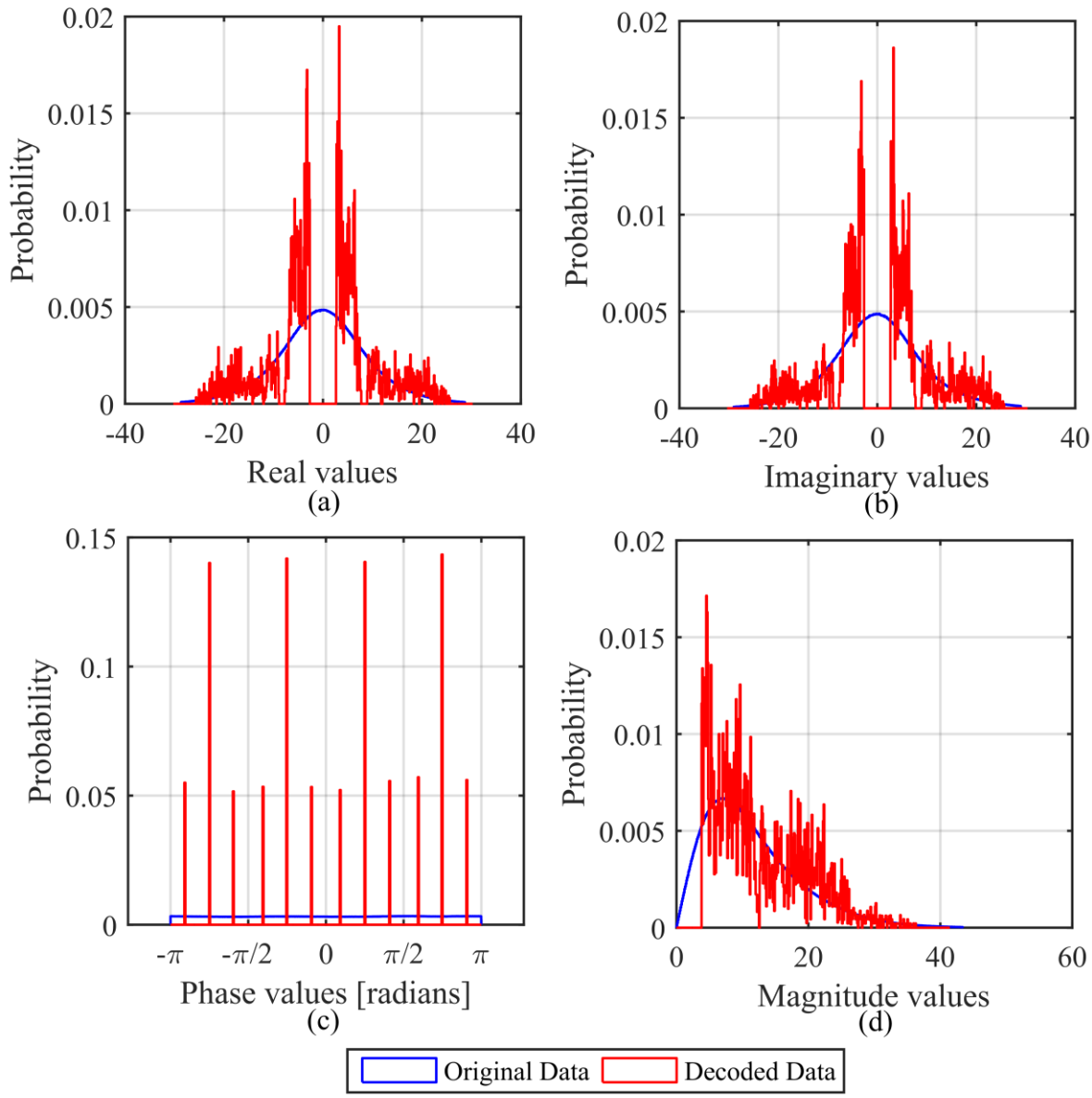

Fig. 4. *Distribution of the data before and after implementing the BAQ algorithm. (a) Real (I) component. (b) Imaginary (Q) component. (c) Phase component. (d) Amplitude component*

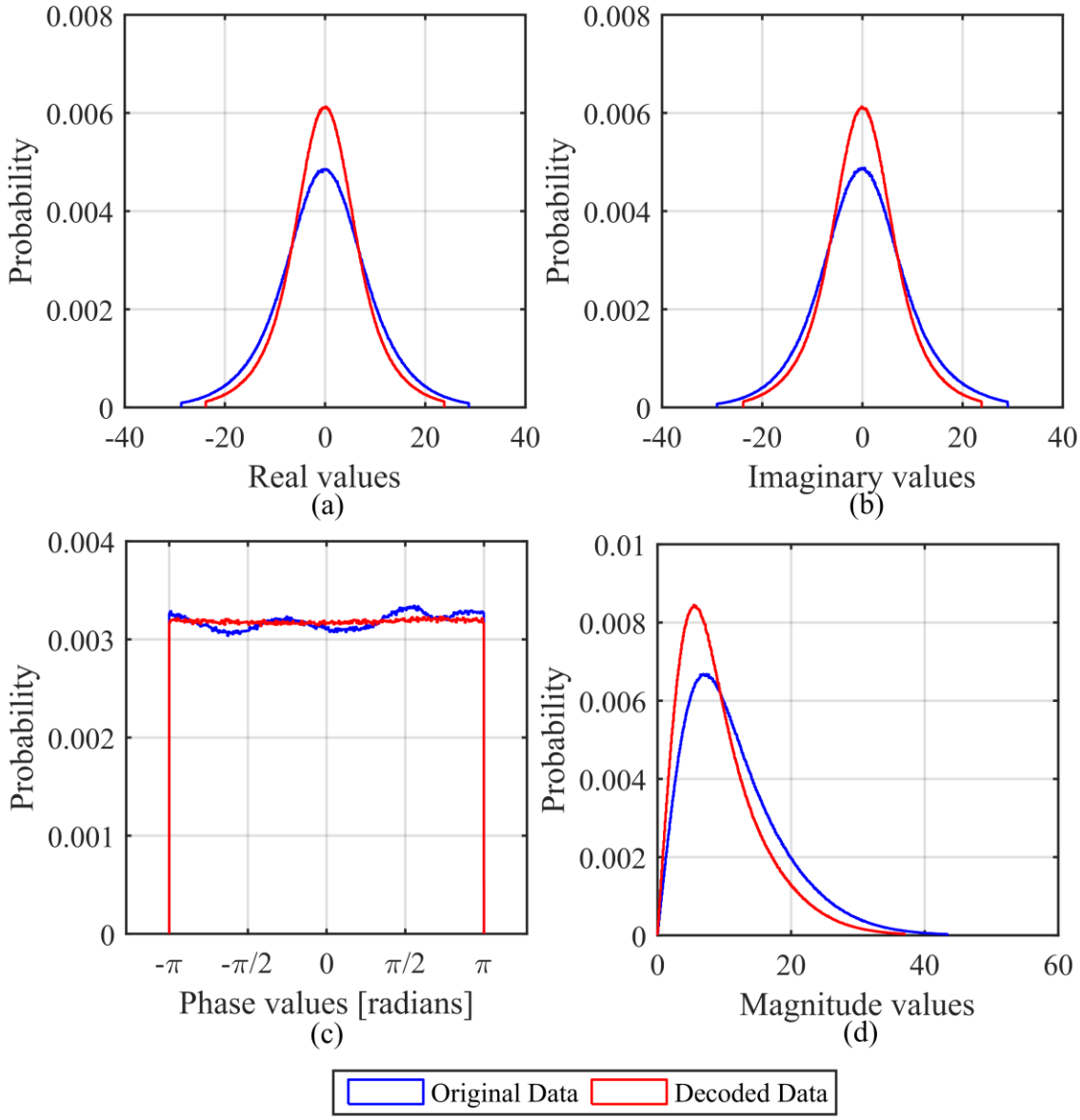

Fig. 5. *Distribution of the data before and after implementing the FFT-BAQ algorithm. (a) Real (I) component. (b) Imaginary (Q) component. (c) Phase component. (d) Amplitude component*

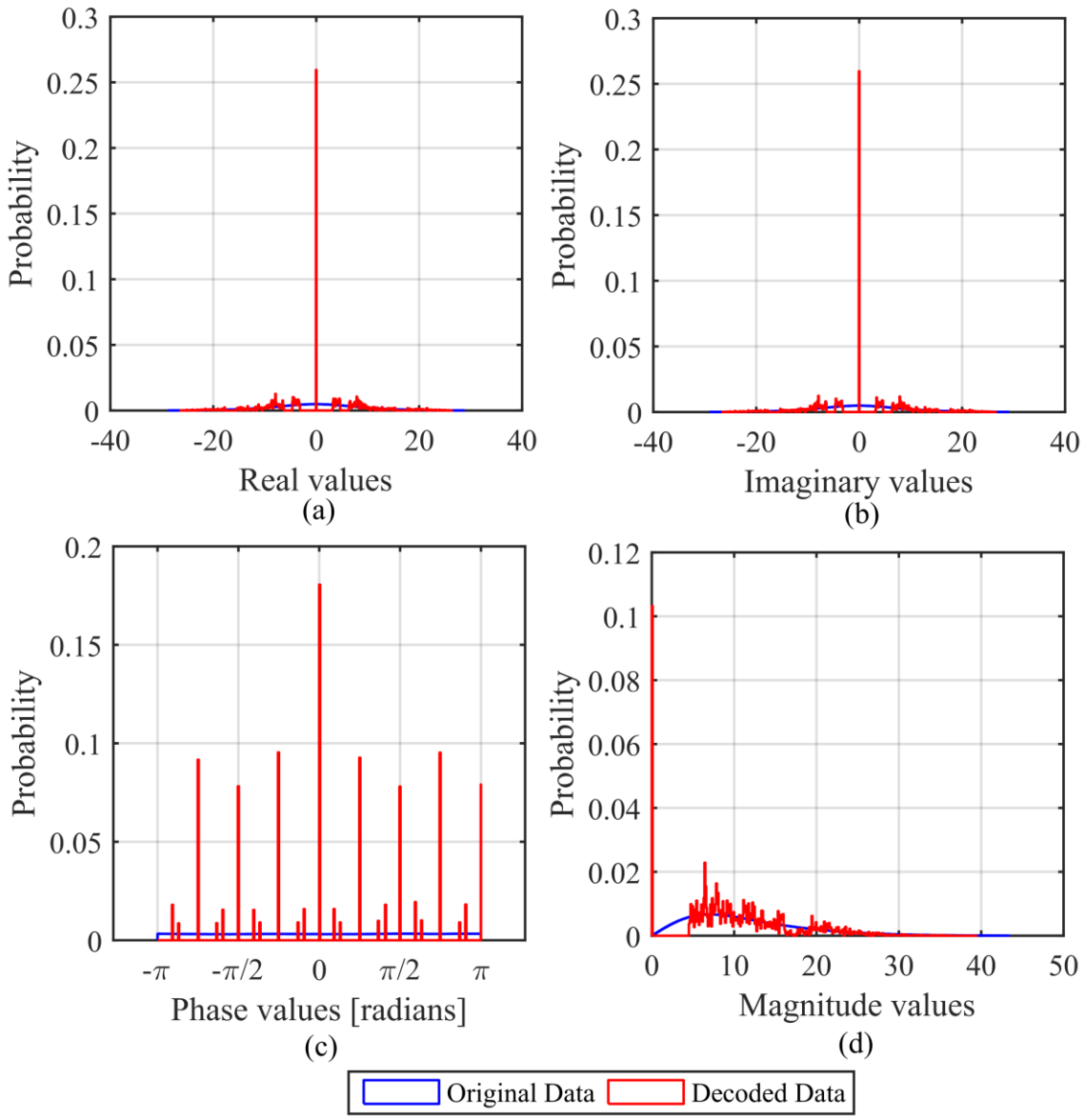

Fig. 6. *Distribution of the data before and after implementing the FDBAQ algorithm. (a) Real (I) component. (b) Imaginary (Q) component. (c) Phase component. (d) Amplitude component*